

## FLEXURAL BEHAVIOR OF SQUARE GEOPOLYMER FERROCEMENT ELEMENTS UNDER UNIFORMLY DISTRIBUTED LOAD

Heiman Said Mohammed Amin <sup>1\*</sup>  and Dilshad Kakasor Ismael <sup>1</sup> 

<sup>1</sup>Department of Civil Engineering, College of Engineering, Salahaddin University, Erbil-IRAQ

### Article History

Received: 25.03.2023

Revised: 27.05.2023

Accepted: 06.06.2023

Communicated by: Dr. Orhan Tug

\*Email address:

[hemin.mohammedamin@su.edu.krd](mailto:hemin.mohammedamin@su.edu.krd)

\*Corresponding Author



Copyright: © 2023 by the author.

Licensee Tishk International

University, Erbil, Iraq. This article is an open access article distributed under the terms and conditions of the Creative Commons Attribution-Noncommercial 2.0 Generic License (CC BY-NC 2.0)

<https://creativecommons.org/licenses/by-nc/2.0/>

### Abstract:

Due to the significant amount of carbon dioxide gas discharged into the atmosphere by the cement industry and the massive amounts of byproduct fly ash also turning into a significant concern. Geopolymers are demonstrating promise in lowering greenhouse gas footprints. The results of testing geopolymer ferrocement elements reinforced with varying numbers of wire mesh layers are presented in this article. The primary objective was to investigate the flexural behavior for geopolymer ferrocement elements by applying a uniformly distributed load by means of a layer of sand. Ferrocements measuring 600\*600\*25 mm were reinforced with 0, 2, 4, 6, and 8 layers of welded square meshes. Test results showed that first crack and ultimate loads increase with increase in wire mesh layers embedded in the ferrocement samples. The element with 6 layers of wire mesh displayed highest deflection. It has been determined that geopolymer ferrocements are versatile materials with excellent deflection capacity along with environmental sustainability.

**Keywords:** Geopolymer; Geopolymer Mortar; Fly Ash; Ferrocement, Applications; Wire Mesh

### 1. Introduction

Ferrocement denotes basically the employment of wire meshes plus cement mortar. Early ferrocement applications include boats and other water-retaining structures. As described by ACI-549; “Ferrocement is a form of reinforced concrete using closely spaced multiple layers of mesh and/or small diameter rods completely infiltrated with, or encapsulated, in mortar. The most common reinforcement is steel mesh”. Figure 1 shows a section of a typical ferrocement element. Ferrocements can have a wide range of applications. Both temporary and permanent buildings have used ferrocement in their construction [1; 2].

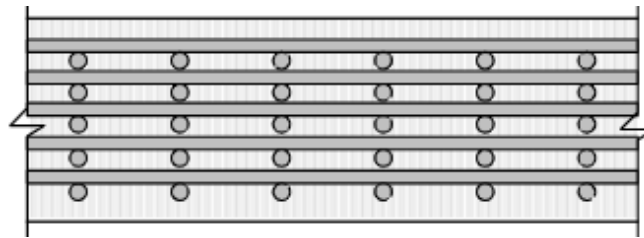


Figure 1: Typical segment of ferrocement with many layers of densely packed welded wire mesh [2]

Due to the substantial quantity of carbon dioxide gas released into the atmosphere by ordinary Portland cement (OPC) concrete, and also the fact that it is becoming increasingly problematic for power plants to dispose of the fly ash they create as a byproduct. In this regard, geopolymers are displaying great potential. Geopolymer concrete/mortar is still a relatively new material and has been developed as a result of the demand for environmentally sustainable concrete for building as there is an increasing trend towards environmental conservation globally [3].

Geopolymer is made of inorganic components (mostly industrial waste matters such as fly ash, slag, etc.) that are pozzolanic in nature and inert until they are activated by an alkali solution during a process known as polymerization (or geopolymerization), which produces materials with good mechanical attributes that mostly depend on the silicate and aluminate ratio, particularly the quantity and concentration of alkaline materials that will react with aluminosilicate to form a gel.

Compared to OPC-based concrete/mortar, geopolymers enjoy better resistance to fire, chemical (acid) attack, corrosion of reinforcement, carbonation, permeation, frost resistance, etc. [4; 5]. These facts make geopolymer employment as the matrix material in ferrocement applications a better alternative to OPC in many circumstances. Hereby, it is intended to experiment on behavior in terms of deflection for geopolymer ferrocement elements (GFEs) in this article.

Despite having many advantages over conventional ferrocement, geopolymer ferrocement is much less widely used. This may be attributed to somewhat lack of widespread availability of basic materials. In reality, the idea of thin elements reinforced with closely spaced continuous uniformly dispersed reinforcing materials is definitely one of the most essential routes to impart excellent crack control to the otherwise brittle mortar matrix, also impart outstanding flexural behavior, and aesthetics. Using geopolymer as matrix material in fabrication of ferrocement gives us a novel material with relatively superior durability. Geopolymer ferrocement has the potential to address the need to use an eco-friendly solution in various applications e.g., linings, pavement slabs, entrances, decorative structures, etc.

## 2. Literature Review

Geopolymer ferrocements do not have a wide array of researches upon them particularly regarding their applications. A number of researchers have experimented on geopolymer ferrocements. Sushma [6] studied folded and trough shaped GFEs.

Sakkarai & Soundarapandian [7] examined how fiber and layers of wire mesh affect a flat and folded geopolymer panel's behavior.

Vinu et al. [8] carried out an experiment to determine the flexural strength of slab elements made of hardened geopolymer concrete and reinforced with several kinds of wire meshes.

A few other authors have also conducted experimental investigations on behavior of geopolymer ferrocements such as Satyanarayana & Patil [9], Baskara Sundararaj et al. [10], Malathy et al. [11], Magudeaswaran et al. [12], and Srikrishna & Rao [13]

### 3. Materials and Methods

Sample GFEs were prepared by installing wire-meshes in molds of defined dimensions to determine their deflection capacity.

#### 3.1 Materials

Fly ash-based geopolymer mortar was prepared. The geopolymer mortar was made using fly ash, fine sand, and a sodium-based alkaline solution ( $\text{NaOH}+\text{Na}_2\text{SiO}_3$ ). Figure 2 illustrates the geopolymer mortar constituent components.



Figure 2: Geopolymer mortar constituent materials

##### 3.1.1 Fly Ash

Fly ash of (Class F) was used as a base for geopolymer binder. The fly ash used was provided by Sika Company and is compliant with BS EN 450 (2005) [14]. The chemical composition of the fly ash shown in Table 1 was issued by the Scientific Research Center of Soran University. The fly ash had a specific gravity of 2.05.

Table 1: Composition of fly ash

Element	Content (%)	Element	Content (%)	Element	Content (%)
MgO	3.9677	Vanadium	0.0047	Zirconium	0.1511
Al <sub>2</sub> O <sub>3</sub>	25.0776	MnO	0.0298	Niobium	0.0061
SiO <sub>2</sub>	60.1602	Fe <sub>2</sub> O <sub>3</sub>	5.5167	Molybdenum	0.0152
P <sub>2</sub> O <sub>5</sub>	0.2506	Cobalt	0.0048	Silver	0.0030
Sulfur	0.2495	Nickel	0.0057	Tantalum	0.0085
K <sub>2</sub> O	0.5423	Zinc	0.0095	Lead	0.0252
CaO	3.5760	Strontium	0.1839	Yttrium	0.0084
TiO <sub>2</sub>	0.2035				

##### 3.1.2 Fine Aggregate

As fine aggregate, locally available natural river sand was utilized to make geopolymer mortar. To make sure that the geopolymer mortar can penetrate the small gaps in between the wire meshes, the

sand was sieved through sieve no. 8 (equivalent to 2.36 mm). The sand particle size distribution depicted in Table 2 complies with ASTM C33/C33M – 18 [15].

Table 2: Fine aggregate size distribution

Sieve No.	Size (mm)	% Passing	% ASTM Permissible
4	4.75	100	95-100
8	2.36	98	80-100
16	1.18	85	50-85
30	0.6	55	25-60
50	0.3	28	5-30
100	0.15	9	0-10
200	0.075	-	0-3
Specific gravity	2.4		
Fineness modulus	2.17		

### 3.1.3 Alkaline Solution

Locally purchased sodium-based solution (a combination of sodium silicate ( $\text{Na}_2\text{SiO}_3$ ) and sodium hydroxide (NaOH) solution) was chosen to be the alkaline activator for geopolymer mortar.

NaOH flakes of 98% purity were used to form 12 M NaOH solution. Commercially available  $\text{Na}_2\text{SiO}_3$  solution with  $\text{SiO}_2/\text{Na}_2\text{O} = 2$  was used with a composition of 14.7%  $\text{Na}_2\text{O}$ , 29.3%  $\text{SiO}_2$  and 56% water.

### 3.1.4 Water

The geopolymer mortar was made easier to work with by using potable tap water. 20% of the fly ash's weight in water was added to the mixture.

### 3.1.5 Wire Mesh

High-quality square welded hot-dipped galvanized steel meshes of 1mm size with apertures of 20\*20 mm and adhering to EN 10143 (2006) & TS EN 10346 made up the wire meshes that were employed (Figure 3). Up to 8 layers were used. The wire-meshes were provided from Gökhangil Co. from Ankara, Türkiye. The characteristics of the welded wire meshes listed in Table 3 were provided by Gökhangil Co.

Table 3: Characteristics of welded wire mesh

Yield Strength	319 N/mm <sup>2</sup>
Tensile Strength	400 N/mm <sup>2</sup>
Density	7900 kg/m <sup>3</sup>
Elastic modulus	194.1 GPa
Elongation at break	24 %



Figure 3: Square welded wire meshes

## 3.2 Methods

### 3.2.1 Mix Proportions

The constituent materials used for geopolymer mortar were determined in adequate proportions. Quantity of fly ash was set at 600 kg/m<sup>3</sup>. The geopolymer mortar mix ratios are shown in Table 4. These ratios were ideal in accordance with various earlier studies on geopolymer mortar/concrete based on fly ash such as in [16–18]. Extra water added for workability purposes was 20% by weight of fly ash. This quantity of water was due to fineness of sand particles (< 2.36 mm) thus having an increased surface area.

Table 4: Geopolymer mortar mix ratios

Geopolymer mortar	Fine aggregates	Sand
	Fly ash: Fine aggregates	1:2
	Alkaline solution: Fly ash	0.45
	Sodium hydroxide molarity	12 M
	Na <sub>2</sub> SiO <sub>3</sub> /NaOH	2.5

### 3.2.2 Sample Preparation, Casting and Curing

For this research, square elements with dimensions of 600\*600\*25 mm were created (Figure 4 and Figure 5) by means of installing differing number of square welded wire meshes in molds (Figure 6) and thus using geopolymer mortar (Figure 7), the GFEs (Figure 8) were casted. The NaOH flakes shall be prepared 24 hours prior to casting by dissolving in water. NaOH solution's molarity was set at 12 M. Otherwise, similar procedure follows for preparation of geopolymer mortar as OPC mortar. The wire-meshes were installed in 0 (control), 2, 4, 6, 8 layers corresponding to volume fractions of wire-mesh reinforcement as 0, 0.63%, 1.26%, 1.89% and 2.51% respectively according to eq. (1) and specific surface of 0, 25.2, 50.4, 75.6 and 100 m<sup>2</sup>/m<sup>3</sup> according to eq. (2) provided in ACI 549.1R-18 [19]. Cover ranging from 2-5 mm in compliance with ACI 549.1R-18. The GFEs were compacted for 1 minute using a vibrating table. Total water/geopolymer solids ratio was 0.39.

$$(1) \quad V_r = \frac{N\pi d_w^2}{4h} \left( \frac{1}{D_{Long.}} + \frac{1}{D_{Trans.}} \right) ,$$

$$(2) \quad S_r = \frac{A_r \text{ in both directions}}{V_c}$$

For square mesh, both directions are equal, so from the above equations, the following can be derived;

$$(3) \quad V_r = \frac{N\pi d_w^2}{2hD},$$

$$(4) \quad S_r = \frac{4V_r}{d_w},$$

Where;

$V_r$  = Volume fraction of reinforcement (wire-mesh),  $N$  = number of wire-mesh layers,  $d_w$  = diameter of wire-mesh,  $h$  = thickness of ferrocement element,  $D$  = center-to-center wire spacing,  $S_r$  = specific surface of reinforcement,  $A_r$  = area of reinforcement,  $V_c$  = volume of composite.

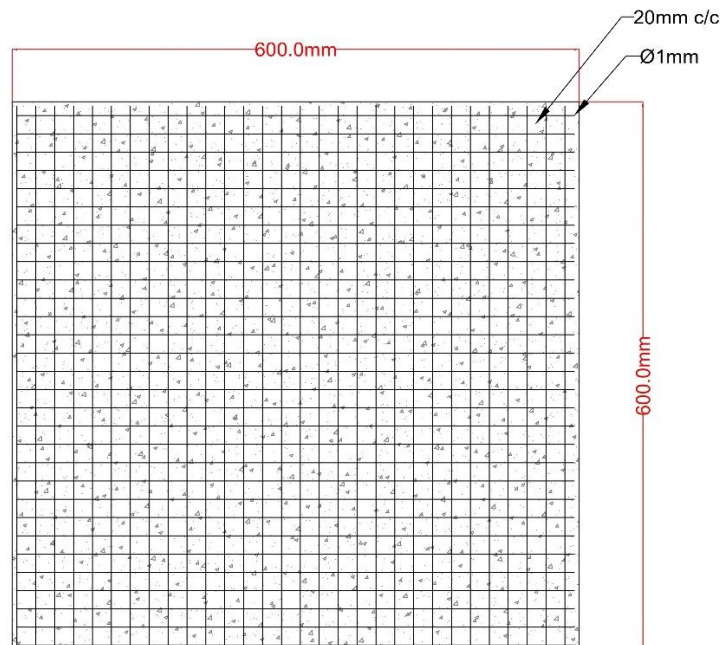


Figure 4: GFE sample model

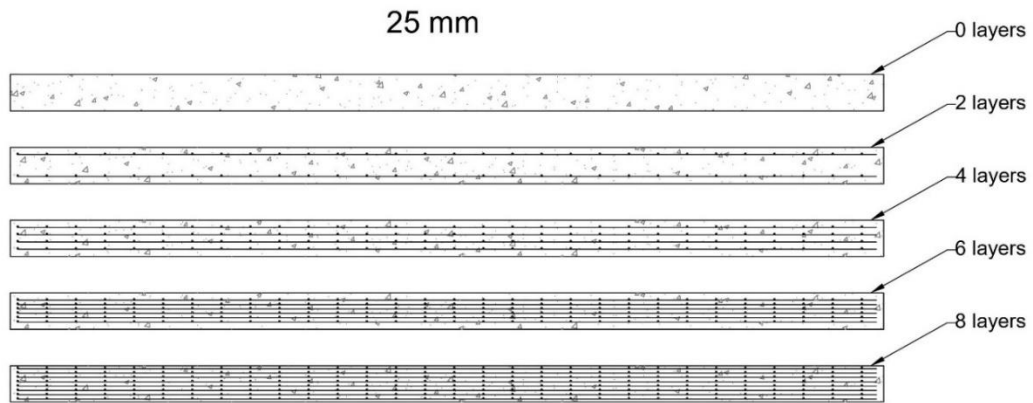


Figure 5: Wire-mesh layers arrangement

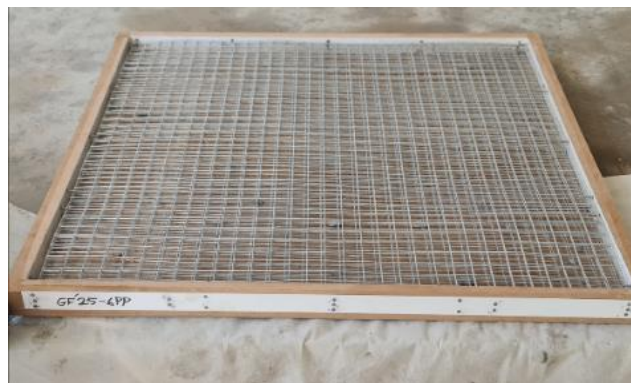


Figure 6: Mold



Figure 7: Geopolymer mortar



Figure 8: Geopolymer ferrocement element

Intermittent heat curing at 60°C was employed for duration of 5 hours for 4 days totaling 20 hours. A heating chamber was used for curing. Prior to curing, a 48-hour rest period was used to slow down the rate of water loss through evaporation so as to prevent excessive shrinkage. The effectiveness of intermittent heat curing has been confirmed by [20]. Table 5 shows the details of the GFE samples. A high temperature during the early stages of curing is necessary to provide the strength needed to attain high mechanical qualities [21].

Table 5: Geopolymer ferrocement sample details

No. of sample	Sample name	Thickness	No. of mesh layers
1	GF25-0	25 mm	0 (control)
2	GF25-2	25 mm	2
3	GF25-4	25 mm	4
4	GF25-6	25 mm	6
5	GF25-8	25 mm	8

### 3.2.3 Experimental Proceedings

#### 3.2.3.1 Setting Time

The initial and final setting durations for the geopolymer mortar used to create the GFEs were determined using a standard Vicat instrument. The ASTM C191-08 [22] procedure was followed. According to ASTM C191, the standard criteria for OPC pastes are that the initial setting time must be at least 45 minutes and the final setting time must not exceed 10 hours. Depending on various conditions, the initial setting timeframes for fly ash-based geopolymer pastes might be much longer.

#### 3.2.3.2 Slump Test

Slump testing was done to determine the flowability and workability of the aforementioned geopolymer mortar. Slump testing was done in accordance with ASTM C143-12 [23] guidelines.

#### 3.2.3.3 Compressive Strength

For testing of compressive strength at ages of 7, 28 and 56 days, 12 (100\*200 mm) cylindrical geopolymer mortar samples were created. Their compressive strength was evaluated using Amsler hydraulic compression machine (Figure 9). ASTM C39-18 [24] guidelines were followed. Capping was done according to ASTM C617-12 [25] by using high-strength stone powder (see Figure 10).



Figure 9: Amsler hydraulic compression machine with capacity of 2000 kN



Figure 10: Capped cylinder samples

#### 3.2.3.4 Split Tensile Strength

The indirect tensile strength of geopolymer mortar, used to cast GFEs, was tested using (100X200 mm) cylindrical samples. Standards outlined in ASTM C496-11 [26] guidelines for splitting tensile strength were followed.

#### 3.2.3.5 Flexural Behavior

The flexural capacity of the ferrocement samples were evaluated using a universal testing instrument. To measure deflection, an LVDT device was mounted on the samples' bottom side. Figure 11 shows the configuration for testing the GFEs. The load was applied in uniformly distributed manner through a layer of sand of 12 cm height on top of each GFE sample. This was achieved by placing a hollow steel base on top of the GFE samples (see Figure 12).



Figure 11: GFE testing configuration



Figure 12: Uniform distribution of load by sand layer

## 4. Results and Discussions

### 4.1 Setting Time

As stated by Ghazy et al. [27], fly ash based geopolymer pastes' ability to set is influenced by a number of variables including the type and concentration of the activator, alkaline activation of fly ash, etc. The silicate to hydroxide ratio in alkaline solution has a strong effect on setting time, also higher alkaline solution to fly ash ratio significantly delays the setting process. Results for initial and final setting times are tabulated in

Table 6. Final setting time took place shortly after initial setting time. The difference between them was only 45 minutes. Due to the various aforementioned conditions, the setting time may have been affected by the alkaline solution to fly ash ratio (0.45) and possibly the proportion of NaO in Na<sub>2</sub>SiO<sub>3</sub>. The relatively high consistency of the geopolymer mortar is also a probable cause for prolonged setting

---

times. Further research is necessary on setting times of geopolymer paste to fully understand the setting process of geopolymer paste.

Table 6: Setting time results for geopolymer paste

Material	NaOH molarity	Na <sub>2</sub> SiO <sub>3</sub> /NaOH	Setting time (min)	
			Initial	Final
Geopolymer paste	12	2.5/1	450	495

#### 4.2 Slump Test

The geopolymer mortar experienced a total collapse with a consistency similar to self-compacting mortar observed. This could be attributed to the fact that geopolymer mortar consisting of fly ash (finer than OPC) and fine sand (< 2.36 mm) in addition to relatively high alkaline solution/fly ash and 20% added extra water by weight of fly ash. T50 and the average diameter from two separate tests were calculated as 4.8 seconds and 660 mm respectively. The average diameter for two separate trials was 60 mm apart. The slump of the mortar is illustrated in Figure 13.



Figure 13: Slump test for the geopolymer mortar

#### 4.3 Compressive Strength

Average compressive strength test results of cylinders for 7, 28 and 56 days are depicted in Figure 14. The samples were heat cured intermittently at 60°C for 5 hours each day for 4 days then left at ambient temperature. Geopolymer mortar averaged 15.5, 18.2 and 36 MPa for 7, 28 and 56 days respectively. Figure 15 shows cracked cylinders under compression. The results showed that there is only slight difference from 7-day to 28-day strength but the strength grew considerably from 28-day to 56-day age.

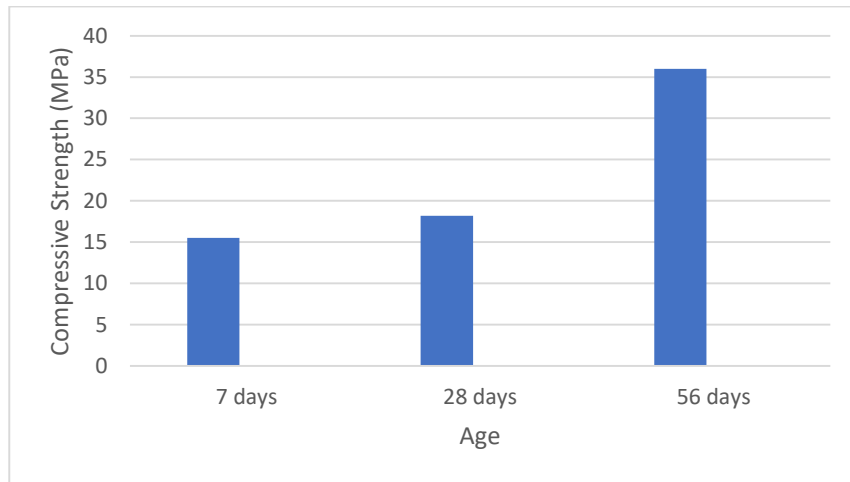


Figure 14: Compressive strength of geopolymer mortar

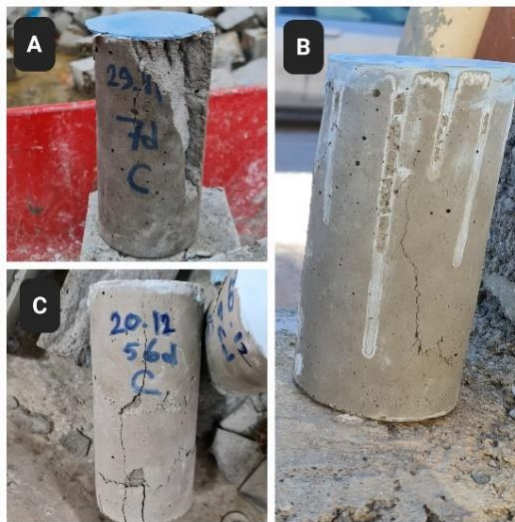


Figure 15: Failure pattern of cylinders under compression at A. 7, B. 28 and C. 56 days

#### 4.4 Split Tensile Strength

Average split tensile strength test results of intermittently heat cured cylinders for 7, 28 and 56 days are depicted in Figure 16. Geopolymer mortar averaged 1.1, 1.42 and 2.07 MPa for 7, 28 and 56 days respectively. Figure 17 shows cracked cylinders under split tensile testing for geopolymer. Same pattern can be seen from compressive test results. The 56-day result is considerably greater compared to the close proximity of 28 and 7-day results.

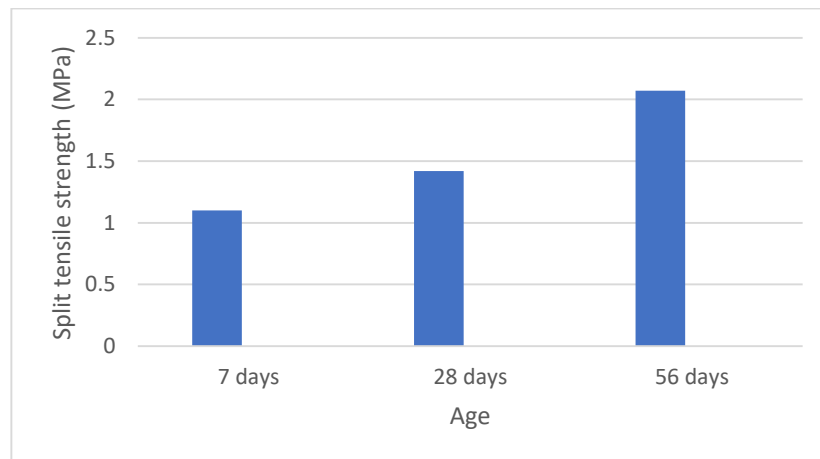


Figure 16: Split tensile strength of geopolymer mortar

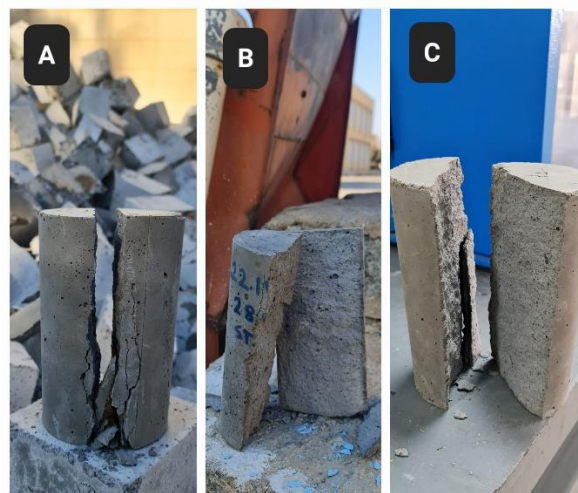


Figure 17: Failure pattern of cylinders under indirect tension at A. 7, B. 28 and C. 56 days

#### 4.5 Flexural Behavior

Weight of the layer of sand was added to the load applied on GFE samples. Results of testing the GFEs have been tabulated in

Table 7. Load-deflection graphs are provided in Figure 18. First crack loads were recorded at the sight of first visible crack at the underside of each sample. The deflections, denoting maximum deflections at failure, were recorded at midspan. Maximum crack widths at failure were measured by means of a set of crack width rulers. With the increase in number of wire mesh layers embedded in the GFEs, both the first crack and ultimate loads went upwards incrementally. Thus, it was observed from the results that number of wire mesh layers had direct impact on the strength of GFEs. Samples with 2, 4, 6 and 8 layers of wire-mesh saw 202.8, 394.4, 497.2 and 536.1% increase in ultimate load respectively. Figure 19 shows percentage increase in ultimate load in terms of control sample. This was not the case regarding maximum deflection. The sample GF25-6 with 6 layers of wire mesh displayed highest deflection. The sample GF25-8 with 8 layers of wire mesh can be considered as possibly having a very dense arrangement of wire meshes with spacing tight for sufficient geopolymer mortar to form a better bond with the meshes. Despite the aforementioned fact, the GFE with 8 layers of wire mesh had highest ultimate load and maximum deflection was still admirable. Samples GF25-2, and GF25-4 also showed decent values in terms of deflection and load capacity.

Table 7: GFE test results

No.	Sample description	Thickness (mm)	No. of wire mesh layers	First crack load (kN)	Ultimate load (kN)	Deflection (mm)	Max. crack width (mm)
1	GF25-0	25	0	2.6	3.6	7	-
2	GF25-2	25	2	3.2	10.9	33	1.00
3	GF25-4	25	4	3.6	17.8	39.7	2.50
4	GF25-6	25	6	3.8	21.5	62.4	4.50
5	GF25-8	25	8	3.7	22.9	48.1	2.50

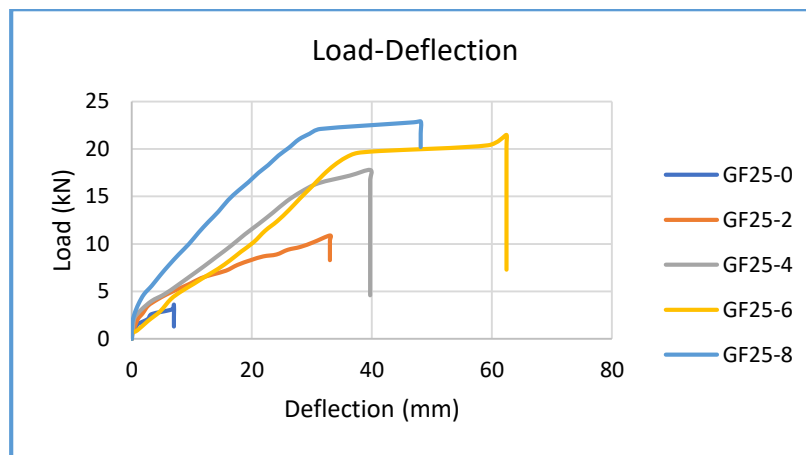


Figure 18: Load-Deflection curves for GFEs

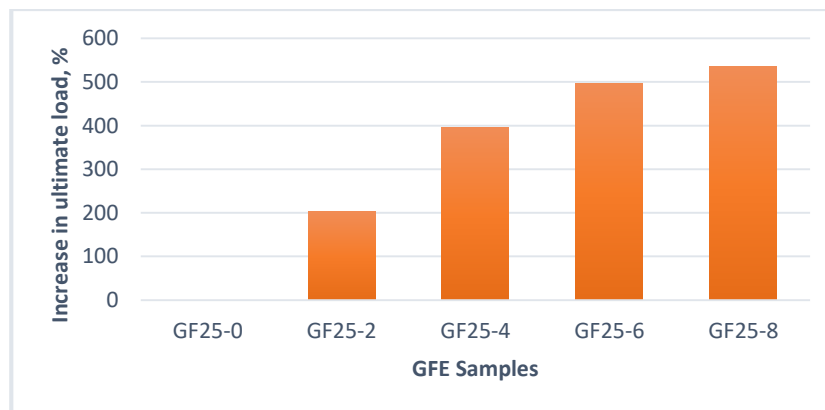


Figure 19: Percentage increase in ultimate load for GFE samples

#### 4.6 Cracking Pattern

The cracking pattern at failure was quite consistent among all the GFE samples. Figure 20 and Figure 21 show the pattern of cracking and the extent of deflection for all the GFE samples used for this experiment. It is apparent that the sample GF25-6 had the greatest extent of deflection at middle. The GFE without embedded wire meshes failed rather quickly after the occurrence of first crack which tended to develop diagonally and disintegrated at failure. The region about the center of the bottom side that was subjected to tensile (flexural) load was where the cracking for the GFEs began (with the exception of the sample with no wire mesh reinforcing). As the deflection grew so did the number of

cracks. At early stages of loading number of cracks increased quite rapidly whereas crack widths increased slowly, but at the latter stages of loading the crack widths increased rapidly particularly just before failure. The cracking pattern eventually took the shape of squares that matched the wire mesh configuration in the samples. The GFEs underwent considerable deflections. This caused the some of the cracks to open more and widen. The failure for sample GF25-6 occurred at the yielding and then snapping of the wire mesh strands at the lowest position due to the high deflection causing crack widening at this position.

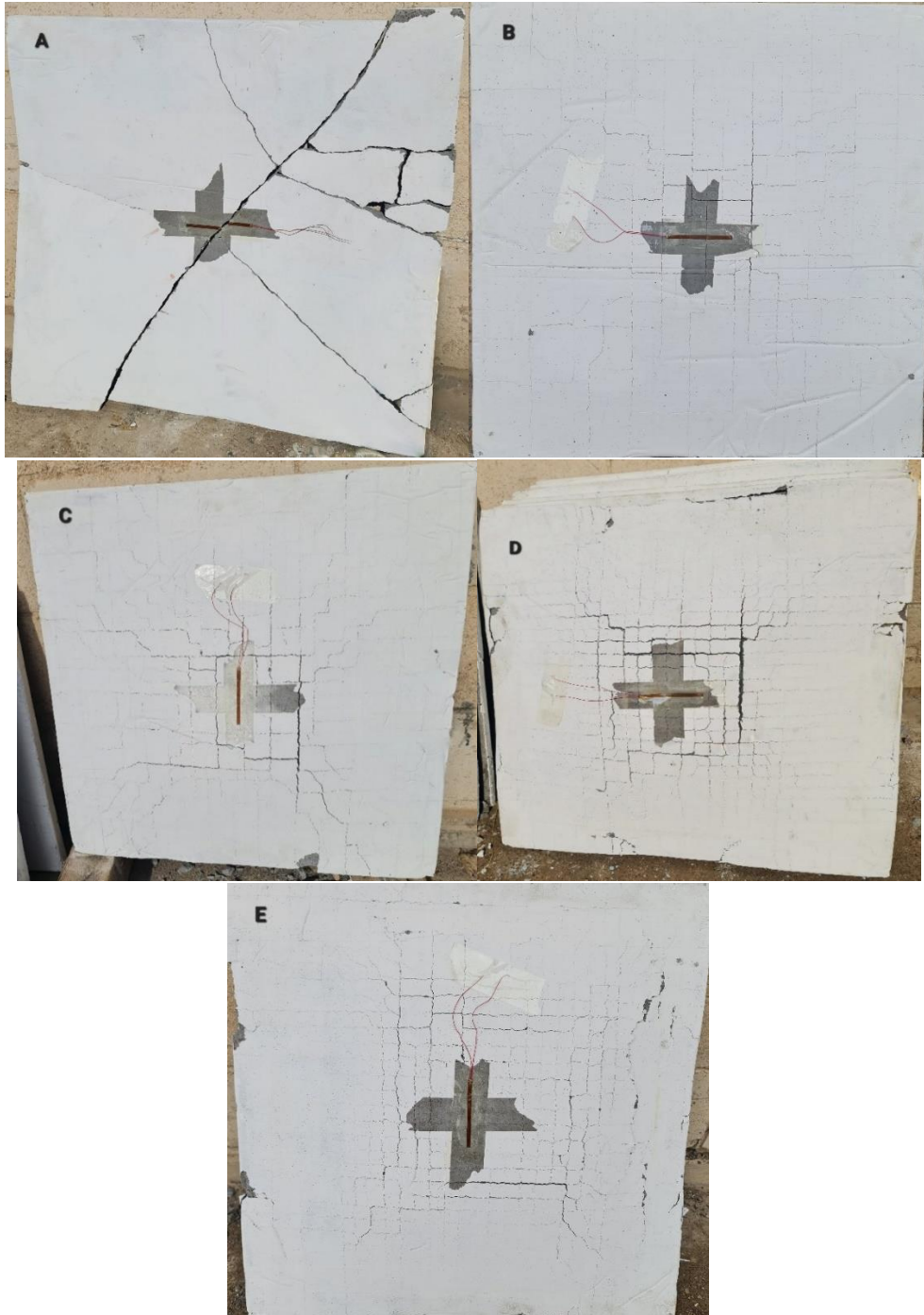


Figure 20: Cracking pattern of GFE samples with A. 0 layers, B. 2 layers, C. 4 layers, D. 6 layers & E. 8 layers of wire mesh



Figure 21: Extent of midpoint deflection of GFE samples with A. 0 layers, B. 2 layers, C. 4 layers, D. 6 layers and E. 8 layers of wire-mesh

## 5. Conclusion

- Ferrocement is a beneficial product. It may be modified to become a potentially superior material in present and future applications by using geopolymers as the binding medium due to enhanced durability and readily available industrial wastes like fly ash and reduced CO<sub>2</sub> emissions.
- Using fine sand and relatively high alkaline solution to fly ash ratio resulted in a geopolymer mortar of high consistency also causing prolonged setting times.
- For compressive and split tensile test results, only a slight increment in strength occurred between 7 and 28 days of age. In contrast, the 56-day results showed a quite remarkable jump in strength.
- The number of layers of wire-mesh employed in the ferrocement elements significantly effects both the flexural loads at the first crack and the ultimate loads.
- The ductility of the components is greatly increased by adding wire-mesh layers, going from 0 to 8 layers.

## 6. Conflict of Interest

There is no conflict of interest for this paper.

## 7. Acknowledgement

This article has been done in partial fulfilment of MSc degree in civil engineering/construction materials at Salahaddin University-Erbil. Special thanks are directed to Civil Engineering Department and the staff of concrete laboratory of the same department for their assistance.

## 8. Authors' contributions

We confirm that the manuscript has been read and approved by all named authors. We also confirm that each author has the same contribution to the paper. We further confirm that the order of authors listed in the manuscript has been approved by all authors.

## References

- [1] Mughal UA, Saleem MA, Abbas S. Comparative study of ferrocement panels reinforced with galvanized iron and polypropylene meshes. *Construction and Building Materials*. 2019; 210: 40–7. <https://doi.org/10.1016/j.conbuildmat.2019.03.147>
  - [2] Naaman AE. FERROCEMENT AND THIN REINFORCED CEMENT COMPOSITES: FIVE DECADES OF PROGRESS. In: Rodriguez C, Bonifacio SN, Naaman AE, Rivas HW, editors. *Proceedings of 12th International Symposium on Ferrocement and Thin Cement Composites*, Belo Horizonte, Brazil: Brasilain Society. 2018; 1–27.
  - [3] Wasim M, Ngo TD, Law D. A state-of-the-art review on the durability of geopolymer concrete for sustainable structures and infrastructure. *Construction and Building Materials*. 2021; 291. <https://doi.org/10.1016/j.conbuildmat.2021.123381>
  - [4] Hongguang W, Lingyu T, Dongpo H, Jianing Z. Durability of geopolymers and geopolymer concretes: A review. *Reviews on Advanced Materials Science*. 2021; 60(1): 1–14. <https://doi.org/10.1515/rams-2021-0002>
  - [5] Zhang X, Long K, Liu W, Li L, Long WJ. Carbonation and Chloride Ions' Penetration of Alkali-Activated Materials: A Review. *Molecules*. 2020; 25(21). <https://doi.org/10.3390/molecules25215074>
  - [6] Sushma P. Experimental Study on Ferro-geopolymer Slab Panels. (IJIRSE) *International Journal of Innovative Research in Science & Engineering*. 2018; 6(1): 29–31.
  - [7] Sakkarai D, Soundarapandian N. Strength Behavior of Flat and Folded Fly Ash-Based Geopolymer Ferrocement Panels under Flexure and Impact. *Advances in Civil Engineering*. 2021; 2021: 1–13. <https://doi.org/10.1155/2021/2311518>
  - [8] Vinu P, Manoli R, Kumar MTP, Kumar KS S. Flexural Behavior of Geopolymer Beam and Slab Elements Reinforced with Different Types of Wire mesh. *IJRST –International Journal for Innovative Research in Science & Technology*. 2016; 3(3): 93–103.
  - [9] Satyanarayana, Patil SG. Properties of ferro-geopolymer mortar slab panels. *International Journal of Innovative Technology and Exploring Engineering*. 2019; 8(12): 1635–41. <https://doi.org/10.35940/ijitee.L3160.1081219>
  - [10] Baskara Sundararaj J, Dhinesh M, Revathi T, Rajamane NP. Comparative Study on Durability, Mechanical Strength and Ecology of Ferrocement Made from Geopolymer and Conventional Portland Cement Mortar. *International Journal of ChemTech Research*. 2017; 10(10): 270–80.
  - [11] Malathy R, Poornima M, Suganthi B. GEOPOLYMER FERROCEMENT PANEL USING FLYASH AND STEEL SLAG. *JASC: Journal of Applied Science and Computations*. 2019; VI(IV): 3667–77.
  - [12] Magudeaswaran P, Palanisamy M, Prakash A, Srikanth T. Durability studies on Geopolymer Mortar Cubes and their Impact Strength characteristics of Geopolymer Ferrocement Panels. *IOP Conference Series: Materials Science and Engineering*. 2021; 1091. <https://doi.org/10.1088/1757-899x/1091/1/012069>
  - [13] Srikrishna TC, Rao TDG. A study on flexural behavior of geopolymer mortar based ferrocement. *Materials Today: Proceedings*. 2020; 43(2): 1503–12. <https://doi.org/10.1016/j.matpr.2020.09.313>
-

- [14] EUROPEAN COMMITTEE FOR STANDARDIZATION. Fly ash for concrete (BS EN 450-2:2005). 2005.
- [15] ASTM C33/C33M – 18. Standard Specification for Concrete Aggregates ASTM C33/C33M – 18. Annual Book of ASTM Standards, 2018. [https://doi.org/10.1520/C0033\\_C0033M-18](https://doi.org/10.1520/C0033_C0033M-18)
- [16] Ojha A, Aggarwal P. Fly Ash Based Geopolymer Concrete: a Comprehensive Review. Silicon. 2021; 14: 2453–72. <https://doi.org/https://doi.org/10.1007/s12633-021-01044-0>.
- [17] Atul, Balasubramanian A, Patil S, Sekar SK. Experimental Investigation on Strength Properties of Geo-polymer Concrete. Cement, Wapno, Beton, 2018. <https://doi.org/10.32047/CWB.2021.26.3.7>
- [18] Hardjito D, Wallah SE, Sumajouw DMJ, Rangan BV. On the development of fly ash-based geopolymer concrete. ACI Materials Journal. 2004; 101(6): 467–72. <https://doi.org/10.14359/13485>
- [19] ACI Committee 549. Design Guide for Ferrocement ACI 549.1R-18. Farmington Hills, MI: 2018.
- [20] Helmy AII. Intermittent curing of fly ash geopolymer mortar. Construction and Building Materials. 2016; 110: 54–64. <https://doi.org/10.1016/j.conbuildmat.2016.02.007>
- [21] Sachet WH, Salman WD. Geopolymer Concrete, Mortar, and Paste: A Review. IOP Conference Series: Materials Science and Engineering. 2021; 1076. <https://doi.org/10.1088/1757-899x/1076/1/012108>
- [22] ASTM International. Standard Test Methods for Time of Setting of Hydraulic Cement by Vicat Needle ASTM C191-08. Annual Book of ASTM Standards. 2008. 04.01: West Conshohocken, PA. <https://doi.org/10.1520/C0191-08>
- [23] ASTM International. Standard Test Method for Slump of Hydraulic-Cement Concrete ASTM C143/C143M-12. Annual Book of ASTM Standards. 2012; 04.02: West Conshohocken, PA. [https://doi.org/10.1520/C0143\\_C0143M-12](https://doi.org/10.1520/C0143_C0143M-12)
- [24] ASTM International. Standard Test Method for Compressive Strength of Cylindrical Concrete Specimens ASTM C39/C39M-18. Annual Book of ASTM Standards, West Conshohocken, PA: 2018. [https://doi.org/10.1520/C0039\\_C0039M-18](https://doi.org/10.1520/C0039_C0039M-18)
- [25] ASTM International. Standard Practice for Capping Cylindrical Concrete Specimens ASTM C617/C617M-12. Annual Book of ASTM Standards, West Conshohocken, PA: 2012. [https://doi.org/10.1520/C0617\\_C0617M-12](https://doi.org/10.1520/C0617_C0617M-12)
- [26] ASTM International. Standard Test Method for Splitting Tensile Strength of Cylindrical Concrete Specimens ASTM C496/C496M-11. Annual Book of ASTM Standards, vol. 04.02, West Conshohocken, PA: 2011. [https://doi.org/10.1520/C0496\\_C0496M-11](https://doi.org/10.1520/C0496_C0496M-11)
- [27] Ghazy MF, Abd Elaty MAA, Abo Elkhair A. SETTING AND MECHANICAL PROPERTIES OF FLY ASH BASED GEOPOLYMERS. International Conference on Advances in Structural and Geotechnical Engineering (ICASGE). 2017; 1–11.
-